Journal of Engineering Science and Technology
Vol. 12, No. 4 (2017) 913 - 934

SEISMIC FRAGILITY ANALYSIS OF IMPROVED RC FRAMES USING DIFFERENT TYPES OF BRACING

HAMED HAMIDI JAMNANI*, GHOLAMREZA ABDOLLAHZADEH, HADI FAGHIHMALEKI

Faculty of Civil Engineering, Babol Noshirvani University of Technology, Iran
*Corresponding Author: h.hamidi@nit.ac.ir

Abstract

Application of bracings to increase the lateral stiffness of building structures is a technique of seismic improvement that engineers frequently have recourse to. Accordingly, investigating the role of bracings in concrete structures along with the development of seismic fragility curves are of overriding concern to civil engineers. In this research, an ordinary RC building, designed according to the 1st edition of Iranian seismic code, was selected for examination. According to FEMA 356 code, this building is considered to be vulnerable. To improve the seismic performance of this building, 3 different types of bracings, which are Concentrically Braced Frames, Eccentrically Braced Frames and Buckling Restrained Frames were employed, and each bracing element was distributed in 3 different locations in the building. The researchers developed fragility curves and utilized 30 earthquake records on the Peak Ground Acceleration seismic intensity scale to carry out a time history analysis. Tow damage scale, including Inter-Story Drifts and Plastic Axial Deformation were also used. The numerical results obtained from this investigation confirm that Plastic Axial Deformation is more reliable than conventional approaches in developing fragility curves for retrofitted frames. In lieu of what is proposed, the researchers selected the suitable damage scale and developed and compared log-normal distribution of fragility curves first for the original and then for the retrofitted building.

Keywords: Fragility curve, Seismic retrofitting, Mid-rise RC frames, Braced frame, Dynamic time history analysis.

1. Introduction

Before a building is hit by an earthquake, there are two possible ways to improve its seismic performance. The first technique is to increase the number of the structural elements of the building, like applying more shear walls or steel braces.

Nomenclatures

R	Response coefficient
T	Period of oscillation, s

Greek Symbols

β	Standard deviation of the seismic intensity scale
φ	Standard Normal Cumulative Distribution
μ	Average value of seismic intensity scale

Abbreviations

APD	Axial Plastic Deformation
BRB	Buckling Restrained Frames
CBF	Concentrically Braced Frames
CFPR	Carbon-Fiber-Reinforced Polymer
CP	Collapse Prevention
EBF	Eccentrically Braced Frames
FRP	Fiber-Reinforced Plastic
IDA	Incremental Dynamic Analysis
IO	Immediate Occupancy
ISD	Inter Story Drift
LS	Life Safety
NLTH	Nonlinear Dynamic Time History Analysis
PGA	Peak Ground Acceleration
PHR	Plastic Hinge Rotation
PL	Performance Level
RC	Reinforced Concrete

The second technique is to improve the performance of inefficient structural elements with concrete or steel covers or by using carbon-fiber-reinforced polymer (CFPR) or fiber-reinforced plastic (FRP) encasements [1 - 5]. In the first technique, concentrically and eccentrically braced frames are used in steel structures, and shear walls are affixed to ordinary reinforced concrete buildings. Nonetheless, in recent years, research has been done on the use of braces to improve the seismic performance of concrete buildings as well [6 - 8].The performance of bracing systems in retrofitting of steel structures was previously studied by some researchers [9, 10], the focus here is to study their performance in RC buildings. Pagni and Lowes [11] developed seismic fragility functions aiming to determine a method for repairing old reinforced concrete (RC) beam-column subassemblies by earthquake loading. Kappos et al. [12] also presented a technique for assessing the vulnerability of reinforced concrete (RC) and unreinforced masonry (URM) structures. Jeong and Elnashai [13] presented an approach whereby a set of fragility relationships with known reliability is derived based on the fundamental response quantities of stiffness, strength and ductility. Lagaros [14] carried out a fragility assessment test on reinforced concrete structures by devising three different methods.

Recently, Kircil and Polat [15] developed fragility curves for mid-rise RC frame buildings in Istanbul, which are, according to Turkey's seismic design code, designed based on numerical simulations in accordance with the number of the stories of the buildings. In their study, Polat and Kirchil designed 3, 5,

and 7 story buildings and employed incremental dynamic analysis (IDA) to measure the yielding and collapse capacity of the designed buildings under twelve artificial ground motions. According to the aptitude of the buildings, they produced fragility curves for the yielding and collapse capacities of the structures under lognormal distribution parameters on the basis of elastic pseudo spectral acceleration, Peak Ground Acceleration (PGA), and elastic spectral displacement. Afterwards, they employed regression analysis to determine the effect of the number of the stories of the buildings on fragility parameters. Their study disclosed that there was a reverse relationship between the number of the stories and fragility parameters.

In this article, the researchers intend to study and evaluate the effect of multiple steel bracings with proper distribution on the improvement of a mid-rise RC frame building's behaviour during seismic activity. To assess the capacity of the studied building to withstand seismic oscillations, nonlinear dynamic time history analysis is carried out and a fragility curve is developed and presented.

2. Developing Fragility Curves By Using Nonlinear Dynamic Time History Analysis

To develop a fragility curve for any kind of building based on nonlinear dynamic time history analysis (NLTHA), it is necessary to consider the following steps:

- Considering multiple buildings as specimen and various kinds of soil as their construction site.
- Calibrating the studied buildings on the basis of the nonlinear behavior of their materials and their deterioration properties.
- Selecting various artificial ground motions recorded from previous earthquakes on the basis of their frequency content and in respect to the soil type of the site, and then scaling them in accordance to various Peak Ground Acceleration (PGA) variables.
- Considering a proper damage scale for the building materials or the frames used, such as "inter story drift (ISD)", "plastic hinge rotation (PHR)", and "axial plastic deformation (APD)".
- Considering a number of acceptable breaking points in accordance to different building design codes.
- Carrying out a nonlinear dynamic time history analysis (NLTHA) for each building regarding different levels of PGA.
- Choosing a proper probability-density function.
- Presenting fragility curves and tables.

3. Damage Scale and Level of Performance During Seismic Activity

To develop fragility curves, it is necessary to use a reasonable damage scale for each structural element. Researchers have extensively studied plastic hinge rotations in beams and columns. In this study, however, inter story drifts and axial plastic deformations in bracing elements are considered as suitable fragility scales to assess the seismic fragility of RC frame structures. Subsequently, to discover which damage scale is more suitable for the bracing frames, the results will be compared. Inter story drift ratio is an important damage demand parameter of building structures under earthquake loads. Consequently, the correct and

convenient evaluation on maximum inter story drift is fairly significant to seismic analysis and design of buildings. Based on the continuous shear-beam model and wave propagation theory [16]. Plastic axial deformation reduces the force that the structural element must resist, provides a fuse to limit actions on other structural elements (e.g., the foundation system) and can provide for significant effective damping [17].

Estekanchi and Arjomandi [18], investigated damage Scales based on a lot of parameters in order to find a correlation between their numerical values. They had compared the selected damage Scales by applying them in the nonlinear analysis of various low rise steel frames subjected to a set of seven earthquake accelerograms corresponding to a specific soil condition. Their results show a relatively satisfactory correlation with maximum drift scale. Some scales such as modal parameters based indexes and plastic ductility index are less satisfactorily correlated to drift index. It is also shown that better correlation between indexes can be achieved by using more comprehensive indexes.

Level of damage to a building can be considered as minimal, moderate and severe, which is often regarded as the performance level (PL) of the building during seismic activities and is treated as a specific seismic hazard level. In the report published by FEMA 306 [19], these three levels of performance are called Immediate Occupancy (IO), Life Safety (LS) and Collapse Prevention (CP), which are the terms employed in this research as well. Hence, the point where damage scale exceeds each of the three damage levels is regarded as system fragility.

4. Modelling and Analysis of the Basic Structure

For this study, a mid-rise RC frame building located in an earthquake-prone region in Iran was selected. The building was residential and designed according to the 1st edition (the oldest version) of Iranian seismic code (known as Standard No. 2800) [20]. It was a five-story building, with ordinary concrete beam-columns frames, without any shear walls. Figure 1 illustrates the ground plan and the intended frame. Central loads are comprised of dead and live loads. Hence, the design load in this study consists of a dead load of 550 kg/m^2. For the ground floor, a live load of 200 kg/m^2 and a roof load of 150 kg/m^2. Other types of loads, such as snow loads or wind loads, were ignored. Furthermore, soil interaction was also overlooked and consequently it was presumed that the columns were perfectly stable in the ground. Story height was also considered to be 3.2 meters.

In the studied building, the compressive strength of concrete was considered to be 210 kg/cm^2 and the thickness of concrete slabs in each story was considered 15 centimeters. Stirrups were also 8 millimeters in diameter and placed 20 centimeters apart in structural elements.

The seismic performance of the studied building was analyzed with SeismoStruct ver.6 [21]. Alike all limited element software, this software is able to perform all linear or non-linear dynamic and static analyses and it has a special efficiency to perform Incremental Dynamic Analysis (IDA). This software was selected as the excellent software in this field in the 15th world conference for earthquake engineering (2012) which was held in Lisbon, Portugal.

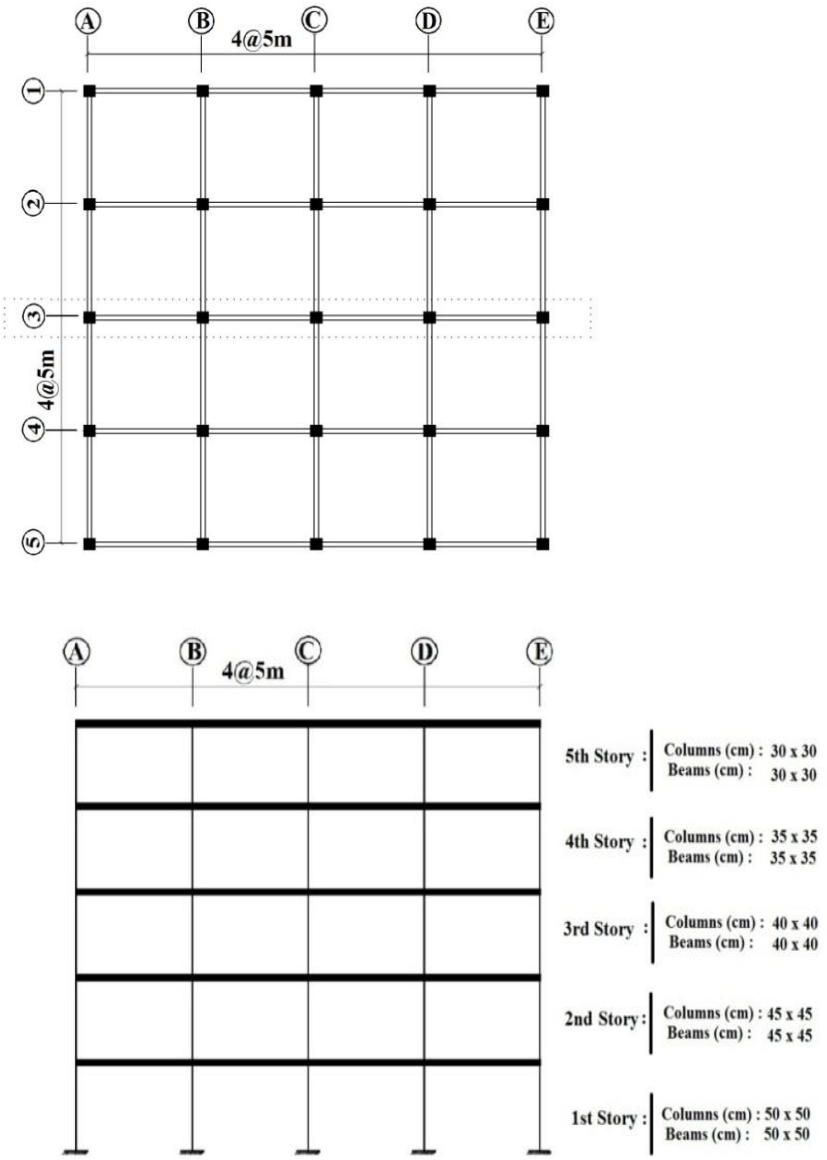

Fig. 1. Story plan and the considered frame (frame No.3) for study.

The quantities of seismic coefficient and seismic shear force were determined according to the 4th edition of Standard No. 2800 [22]. On the second evaluation of the specimen according to the same standard, it was observed that tensile strain exceeded the allowable tensile limit in the aforementioned building design code. The results demonstrate that, based on the 4th edition of Standard No. 2800 and Iranian National Building Code [23], the building lacks lateral resistance and is in need of a retrofitting, Fig. 2, Eqs. (1) to (3).

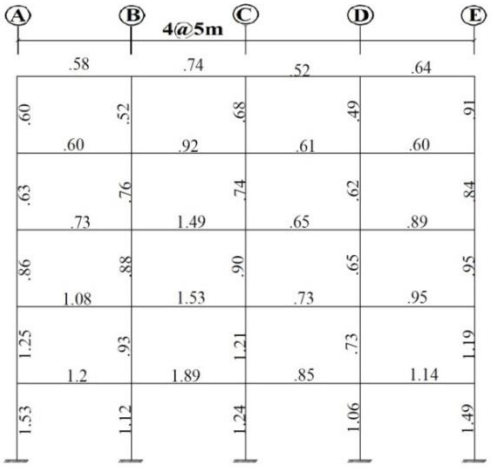

Fig. 2. Unacceptable tension limits in the proposed framework (frame. 3).

According to the seismic design code in the 4th edition of the Iranian seismic code (Standard 2800), story drift should not exceed this amount:

$$T \leq 0.7(\text{Sec}) \rightarrow Drift < \frac{0.0357}{R} \quad (1)$$

$$T \geq 0.7(Sec) \rightarrow Drift < \frac{0.0286}{R} \quad (2)$$

where T is the period of oscillation (seconds) and R is response coefficient. So in this study the following equation is obtained:

$$T \leq 0.7(Sec) \rightarrow Drift = 7.23 \times 10^{-3} > 5.1 \times 10^{-3} \rightarrow \textit{unacceptable story drift} \quad (3)$$

According to FEMA 356 code [24], buildings designed and structured based on the 4th edition of the Standard No. 2800, do not need seismic evaluation or retrofitting. Yet, in this study, it is revealed that according to the level of seismic hazard and the expected structure survivability, the proposed RC building indeed needs seismic retrofitting. Some modifications to the 4th edition of Iranian seismic standard has resulted in a slight variance in the calculated amount of seismic lateral force, and as a result, buildings designed based on the 1st edition of Iranian standard code do not fit in to the standard codes of the 4th edition and thus require a retrofitting.

5. Retrofitted Structures

It is vitally important to develop efficient retrofitting systems to improve the seismic performance of RC buildings before these structures are exposed to earthquakes [25, 26]. In this study, three different types of bracings that are Concentrically Braced Frames (CBF), Eccentrically Braced Frames (EBF) and Buckling Restrained Frames (BRB) were employed. Each bracing element was distributed in three different locations in the building to reach the best level of seismic performance. The various types of concentrically braced frames, eccentrically braced frames and buckling restrained frames are named, respectively, C1, C2, C3, E1, E2, E3 and B1, B2, B3. Figure 3 illustrates a mid-rise RC frame retrofitted with different types of bracings each distributed variously.

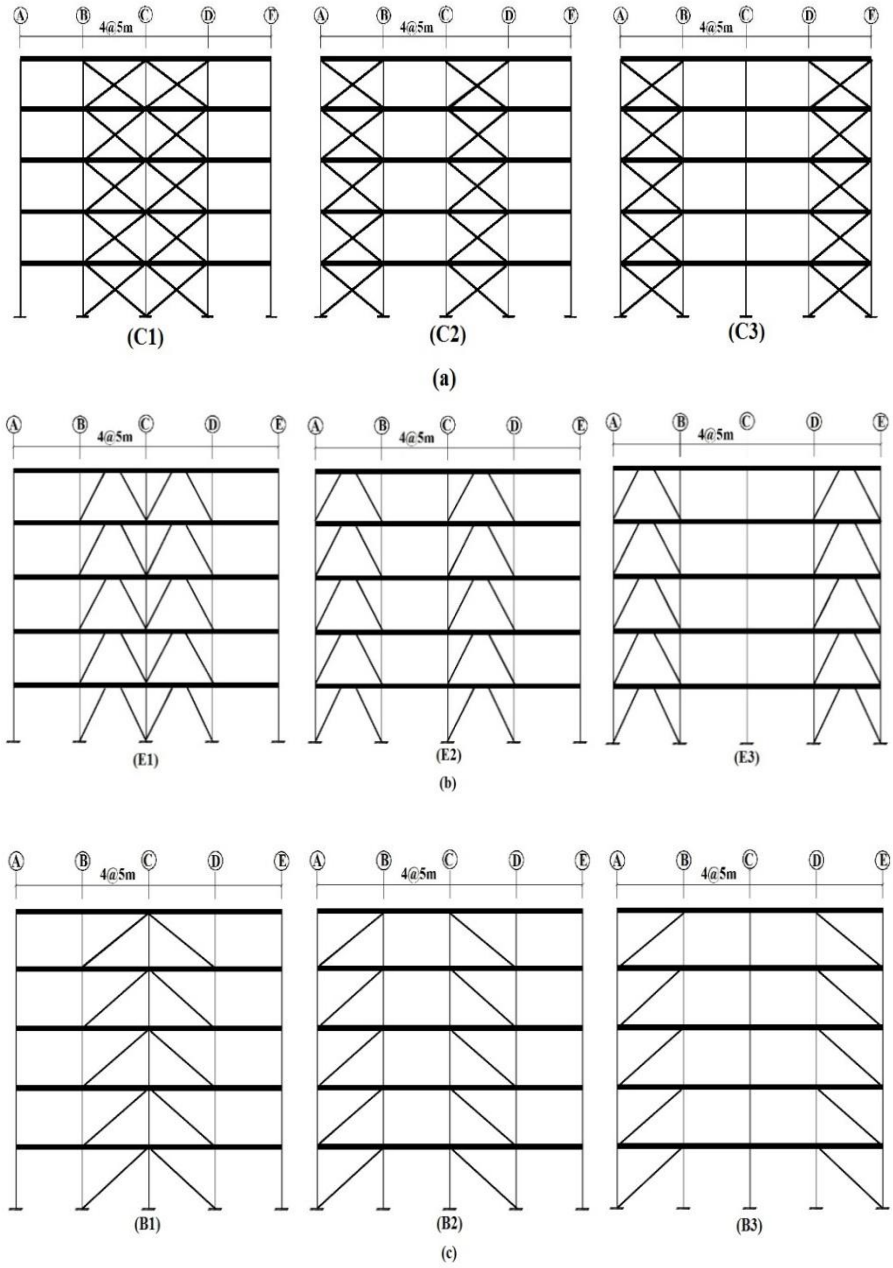

Fig. 3. Seismic retrofitting of the intended mid-rise RC frame with a) CBF; b) EBF; and c) BRB.

5.1. Buckling restrained braces (BRB)

One of the shortcomings of current buckling restrained braces is a mismatch between their tensile and compressive strengths which results in the failure of the bracing system in cyclic loadings [27]. However, in unbounded braces the core is

designed so as to yield in both compression and traction. To prevent buckling of the whole structure under compressive force, the core is encased with a steel tube and confined with mortar or concrete infill. Before adding mortar, an inbounding material fills the empty space. In Fig. 4, the hysteric behavior of ordinary braces is compared to that of BRBs. If the buckling resistant mechanism has proper dimensions, the core displays regular hysteric behavior under the forces applied, either compression or traction, even up to 2% strain [28].

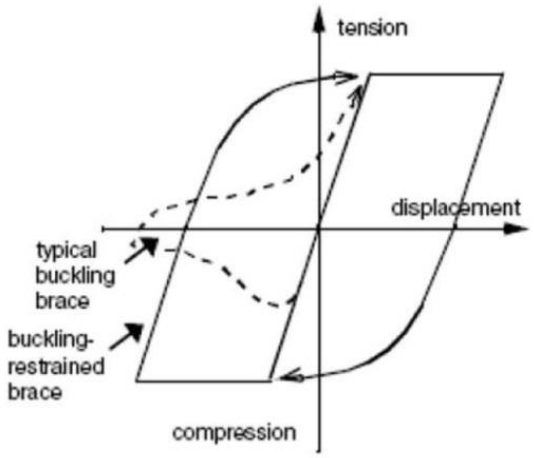

Fig. 4. Comparison between the hysteric behaviors of ordinary braces with BRB [29].

In this research, the size of the core, the tube, and the thickness of the cover of BRB are 153×19(mm2), 200×71(mm2) and 3 mm, respectively. The core is made of ST37mild steel and the external encasing cover is ST52 high-carbon steel. The concrete used in this research is ordinary concrete with a compressive strength of 21 MPa. There is also a 2.5 mm space between the core and the concrete infill from all sides. The space mentioned is the same as the thickness of the isolator. A layer as isolator is used to ensure the core reaches higher modalities under pressure and due to the existence of bracings, exhibits a better behavior under cyclic loading. In this model, the infill concrete and the steel cover are adjacent and in contact with each other.

5.2. CBF and EBF braces

Concentrically Braced Frames (CBF) and Eccentrically Braced Frames (EBF) elements in the studied building all share the same cross-section size and material on each story. In this piece of research, bracing elements are hollow rectangular sections, 15 cm wide and 4 mm thick (Fig. 5). Therefore, all these braces have medium thickness and their effective length coefficient is equal one. Especial attention has also been given to the points where steel braces and reinforced concrete elements meet the shear joints. Various experiments and theoretical studies have also been carried out on the question of joints [30, 31].

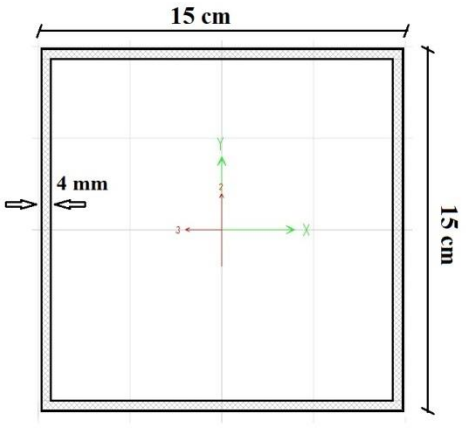

Fig. 5. CFB and EBF element cross-section.

6. Nonlinear Time History Analysis

A nonlinear time history analysis was carried out and the seismic responses of the original and the retrofitted structures were calculated and fragility curves were developed. Beams and columns were modeled as nonlinear frame elements with plastic joints on their two ends (using fiber model). Takeda and Kinematic stress-strain models have been used for concrete and steel materials respectively. Afterwards, SeismoStruct ver. 6 was employed to investigate the seismic behavior of the structure. The vibration records utilized in this research are shown in Table 1 (taken from PEER institute's database [32]). Researchers in this study utilized30 vibration records with magnitudes varying from 6.5 to 7. They also selected grade C and D soil for analysis, and assumed the distance between the epicenter and the construction site to be 15 to 30 Kilometers. Ground acceleration value from each vibration was also calculated, converted and then filtered with SeismoSignal ver. 5.1 [33].

7. Developing Fragility Curves

Fragility curves are one of the critical parameters in assessing earthquake hazards, and determining the potential seismic performance of various structures. In other words, fragility curves are used to illustrate how much ordinary concrete buildings and retrofitted structures are vulnerable and prone to failure during seismic activities. As a result, it can be argued that fragility curves are statistical tools that demonstrate the probability of reaching or exceeding a given damage scale (here different levels of FEMA 306 codes are intended) with the use of seismic intensity scale (here PGA is intended). This probability can be calculated by using the following equation:

$$P[\,D = X\,] = \varphi\,[\,\frac{1}{\beta} ln\left(\frac{X}{\mu}\right)\,] \tag{4}$$

where φ is standard normal cumulative distribution, X is the lognormal seismic intensity scale, and μ is the average value of seismic intensity scale defined with the use of acceptable drift ratios at which point the structure reaches the damage state. β is also standard deviation of the seismic intensity scale's natural logarithm at

different damage levels. To determine β and μ, it is obligatory to carry out a nonlinear time history analysis for each structure and obtain a group of maximum damage scales on the PGA scale. PGA of course, is not the best measure "to describe the intensity of strong ground motion". For one reason, it fails "to provide information about the frequency content or duration of earthquakes". However, it is preferred here, because it is simple to calculate and there is no other alternative for measuring nonlinear dynamic processes without strength degradation [34].

Table 1. Characteristics of the recorded vibration signals used.

Record ID	Earthquake Name	Station	Peak Ground Acceleration (g)	Peak Ground Velocity (cm/s)	Peak Ground Displacement (cm)
P0810	Cape Mendocino	Rio Dell	0.385	43.9	22.03
P0345	Coalinga	Park Field	0.112	14.6	5.69
P0817	Landers	Morongo Valley	0.188	16.6	9.45
P0739	Loma Prieta	Halls Valley	0.134	15.4	3.3
P0889	Northridge	Beverly Hills	0.617	4.8	8.57
P0058	San Fernando	Lake Hughes	0.145	17.3	2.88
P0139	Tabas	Boshrooyeh	0.107	13.7	10.5
P0360	Coalinga	Vineyard Cany	0.23	27.6	6.21
P0352	Coalinga	Gold Hill	0.094	11.0	2.87
P0891	Northridge	Big Tujunga	0.245	12.7	1.12
P0933	Northridge	Sunland	0.157	14.5	4.29
P0166	Imperial Valley	Chihuahua	0.27	24.9	9.08
P0169	Imperial Valley	Cucapah	0.309	36.3	10.44
P0916	Northridge	La Crescenta	.159	11.3	3.0
P0899	Northridge	Glendale	0.357	12.3	1.94
P0808	Cape Mendocino	Fortuna	0.116	30.0	27.59
P0323	Coalinga	Cantua Creek	0.281	25.8	3.71
P0168	Imperial Valley	Compuertas	0.186	13.9	2.92
P1547	Duzce	Bolu	0.822	62.1	13.55
P0164	Imperial Valley	Calipatria Fire	0.128	15.4	10.91
P0173	Imperial Valley	El Centro Array	0.139	16.0	9.96
P0814	Landers	Desert Hot	0.171	20.2	13.87
P0818	Landers	North Palm	0.134	14.5	5.57
P0747	Loma Prieta	Hollister Diff.	0.279	35.6	13.05
P0743	Loma Prieta	Anderson Dam	0.244	20.3	7.73
P0792	Loma Prieta	WAHO	0.638	38.0	5.85
P0892	Northridge	Canoga Park	0.489	14.2	5.5
P0721	Superstitn Hills	Plaster City	0.186	20.6	5.4
P0722	Superstitn Hills	Wildlife Liquef.	0.408	6.0	3.9
P0914	Northridge	LA - Saturn St	0.474	34.6	6.55

Initially, the paper compares two damage scales of "Inter-Story Drifts" and "Plastic Axial Deformation" for bracing elements. To this aim, fragility parameters of the retrofitted frame C1, were determined on both damage scales. The fragility curves obtained are presented in Fig. 6.

The variance between fragility curves in Figs. 6(a) and 6(b) proves that the damage scales used in this experiment do not yield similar damage scales. In fact, in comparison to plastic axial deformation, inter-story drift as damage scale yields lower fragility measures. So it can be claimed that inter-story drift as damage scale is not reliable in fragility analysis of braced frames. This fact is expressed in FEMA 356 as well. In this report, a more meticulous analysis is provided for plastic axial deformation than for inter story drift. In lieu of these results, plastic axial deformation is employed in this research as damage scale for bracing elements and fragility curves for the original and retrofitted frames are developed and compared as follows. Jamnani et al. [35] also developed fragility curves for X-braces in reinforced concrete buildings with a specific damage scale. Standard deviation and average seismic intensity scales for various damage levels were estimated through linear regression. Figure 7 illustrates the linear regression for one type of brace and the original building. This figure shows that correlation coefficient R2 sways from 0.91 to 0.97, which is the indication of a suitable linear relationship.

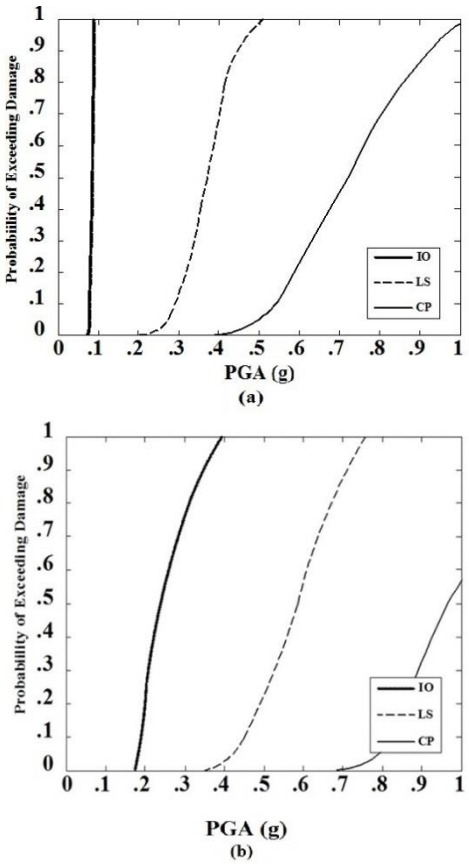

Fig. 6. Fragility curves for C1 frame and two damage scales for bracing elements; a) Plastic axial deformation and b) Inter-story drifts.

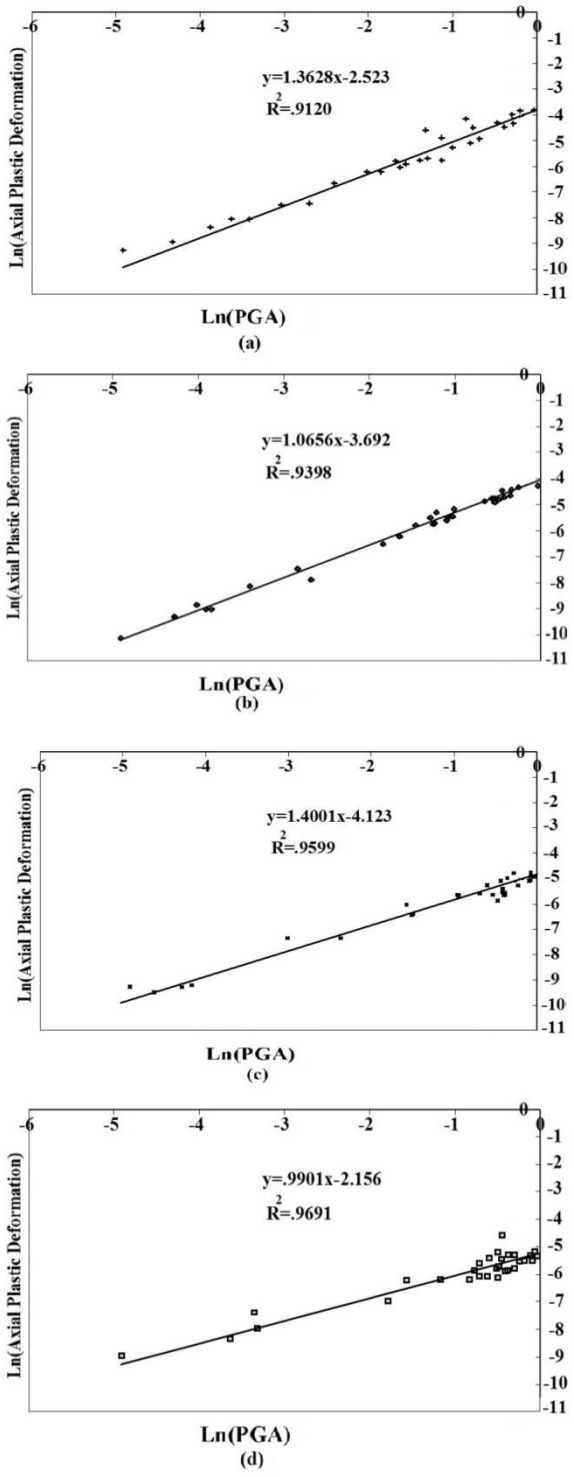

Fig. 7. Linear regression (a); original frame (b) and retrofitted frame C1, (c) E1 and (d) B1.

In Table 2, the two parameters of fragility curves of standard deviation and the average lognormal seismic intensity scale are shown on the basis of PGA for various damage scales.

Table 2. Fragility parameters.

Building Type		Damage Level					
		IO		LS		CP	
		μ	β	μ	β	μ	β
Original	O	0.0544	0.466	0.362	0.377	0.426	0.417
CBF Brace Frame	C1	0.0625	0.515	0.423	0.737	0.641	0.809
	C2	0.0797	0.731	0.530	0.685	0.836	0.601
	C3	0.0920	0.0453	0.625	0.700	0.841	0.523
EBF Brace Frame	E1	0.9253	0.236	0.753	0.412	0.886	0.900
	E2	0.9296	0.456	0.781	0.400	0.890	0.520
	E3	0.9310	0.136	0.790	0.563	0.926	0.369
BRB Brace Frame	B1	0.9566	0.691	0.812	0.236	0.962	0.539
	B2	0.9601	0.520	0.923	0.201	0.980	0.620
	B3	0.9621	0.369	0.936	0.206	0.983	0.428

Various fragility curves developed for the original and retrofitted buildings are presented in Figs. 8 to 11. This study reveals that fragility curves for all damage scales used in this study have similar graphs and only different amounts. This fact proves that performance level of the building (such as Immediate Occupancy (IO), Life Safety (LS), and Collapse Prevention (CP)) improves significantly after a retrofitting. Moreover, under the same strength seismic vibration, retrofitted structures exhibit a lower damage scale.

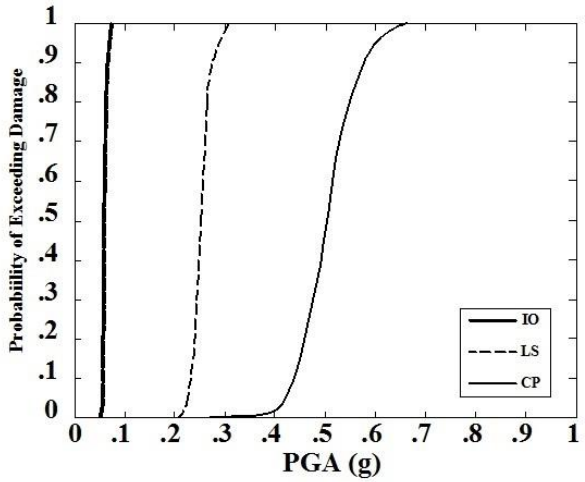

Fig. 8. Fragility curve of the original building with different damage scales.

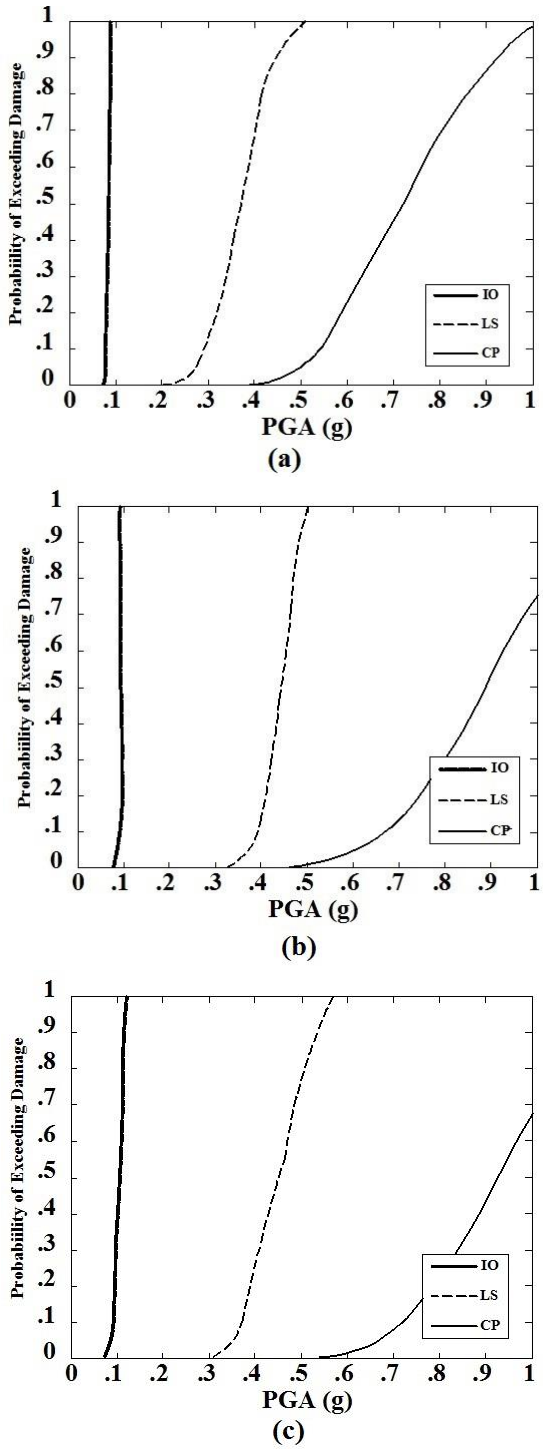

Fig. 9. Fragility curves of the CBF with different damage scales; (a) model C1; (b) model C2 and (c) model C3.

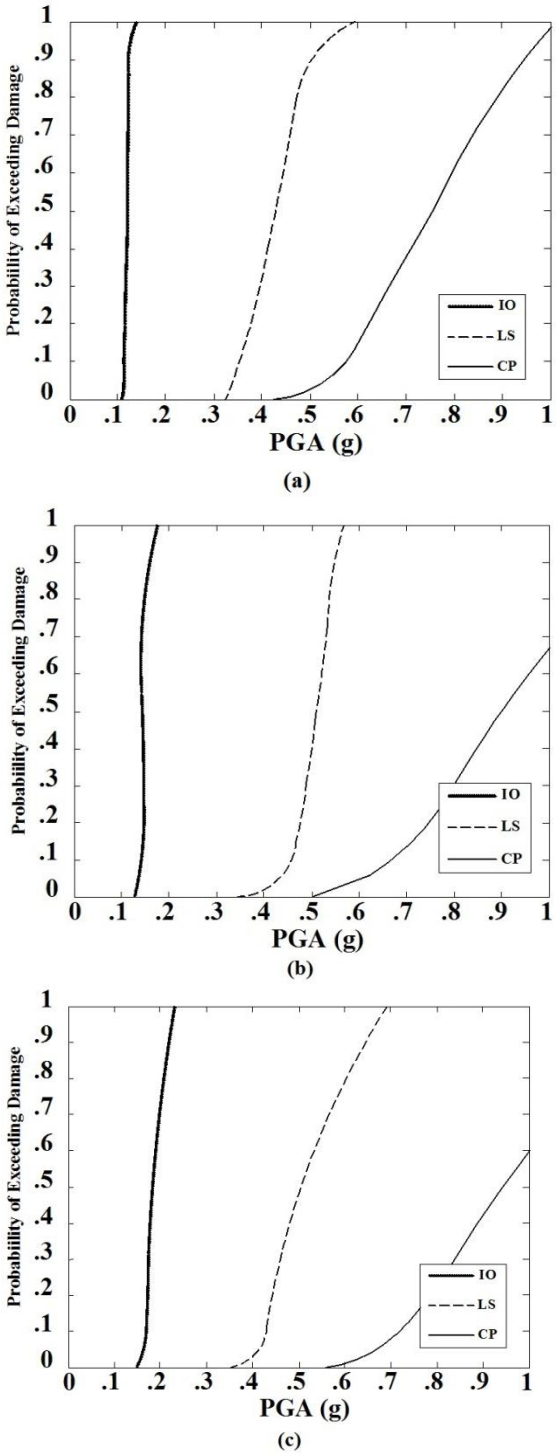

Fig. 10. Fragility curves of EBF with different damage scales; (a) model E1; (b) model E2 and (c) model E3.

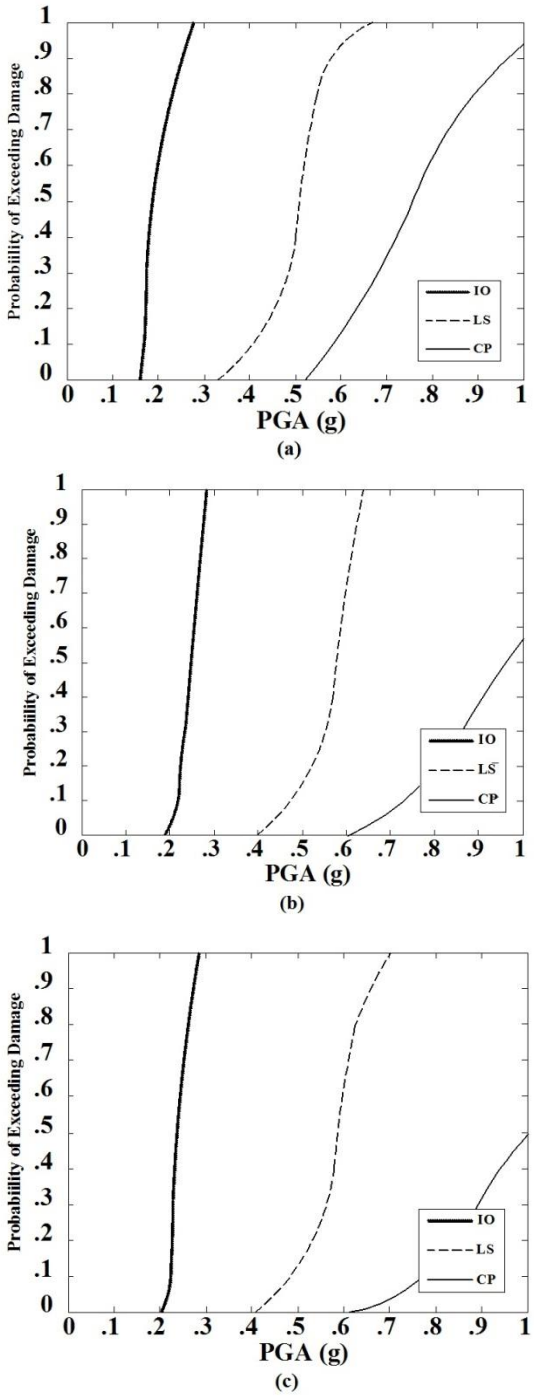

Fig. 11. Fragility curves of BRB with different damage scales; (a) model B1; (b) model B2 and (c) model B3.

The fragility curves of the original and the retrofitted frames explain that; first, when the force and intensity of the vibrations start to build up, damage scale of the buildings begins to fluctuate, until each building has to tackle the maximum level of seismic intensity it can resist and then collapses; second, with slight PGA modifications, damage level alters substantially, which is the sign of response amplitude uncertainty. Response amplitude uncertainty increases as PGA increases and as a result nonlinear movements escalate.

Regarding the fact that distribution of braces is just slightly different for each type, it is only necessary to calculate standard deviation and average fragility parameters [see Table 2] to compare their functionality. With this intention, fragility curves are developed for each single damage scale, as can be seen in Fig. 12, which proves the functionality and efficiency of the braces used. As the figures indicate, when damage scale boosts, the braces act consummately and increase the seismic performance of the building.

From this fact it can be concluded that, C3, E3, and B3 frames perform most competently under various load distributions during seismic activities. These frames, during seismic activities of the same strength, are less likely to collapse when damage scale is high (CP for instance). This fact can be generalized about all other damage scales. Load distribution in these braces is symmetrical and in maximum distance. As a result, the anchor becomes more robust when torsion increases and the distance between the center of stiffness and the center of mass is minimized and so there are no torsions in the floor plan as a result of an earthquake and the frames perform reliably.

From among the three models preferred (which means C3, E3 and B3), the fragility curves show that B3 is the best bracing type. B3 employs BRB and therefore its hysteric behavior is the same under pressure or compression (see Fig. 4), and consequently it has a better seismic performance. Furthermore, the comparison of the fragility curves of C3 and E3 shows that E3 performs better than C3 under seismic activity, for it uses EBF. EBFs absorb more seismic energy than CBFs, and consequently, destructive forces (such as kinetic and potential energies) are reduced in eccentrically braced frames.

Abdollahzadeh and Faghihmaleki [36] have amply analyzed and evaluated the performance of both steel and concrete BRBs and EBFs and compared the amount of energy they absorb to the original amount of seismic force exerted on the braces. Furthermore, Faghihmaleki et al. [37] have analyzed the effect of structure height in seismic fragility curve. Peak ground acceleration is estimated as 0.22 to 0.39 for the IO level of performance. For LS level, this amount reaches 0.29 to 0.57 and for CP it hits at least 0.41.

It is also evident that for average vibration intensity at each level, the changes in retrofitted frames are puny. To better understand the consequences of brace distribution, a histogram is used to illustrate the average probability of exceeding the allowable limit (see Fig. 13).

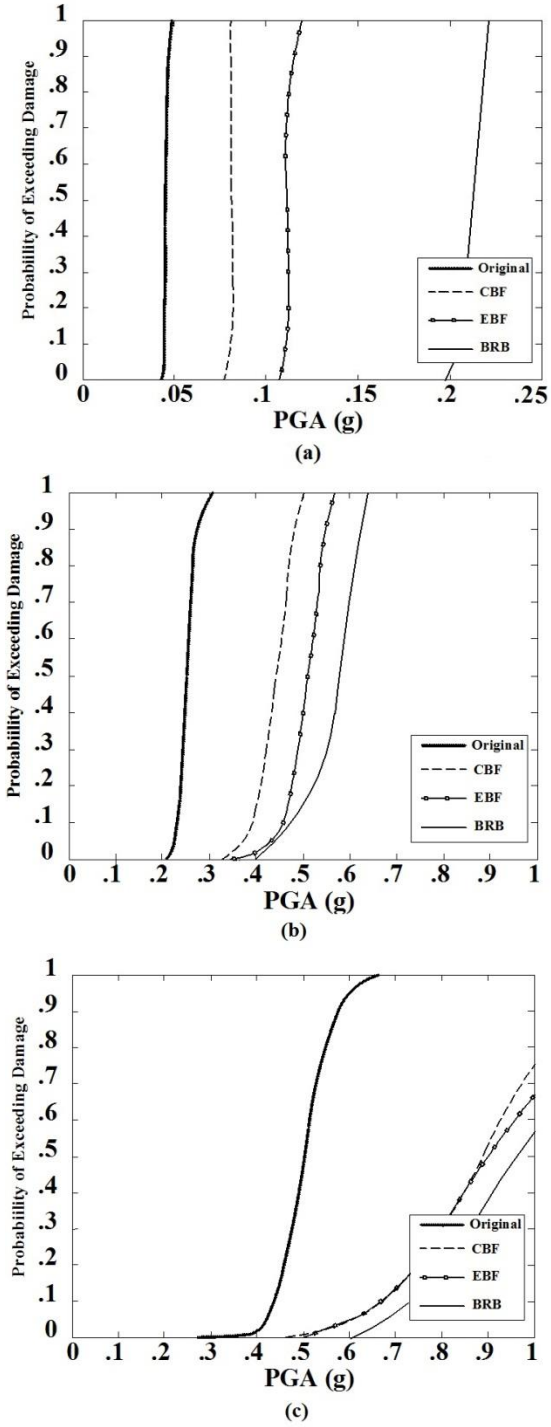

Fig. 12. Comparison of fragility curves of the original and braced frames with performance levels of;(a) IO, (b) LS and (c) CP.

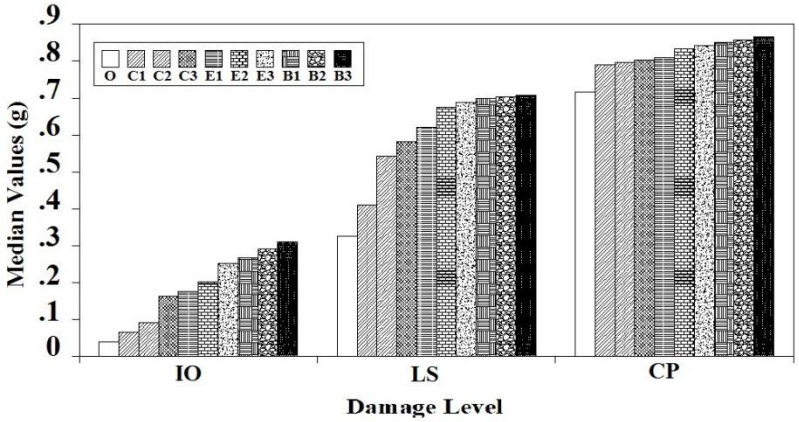

Fig. 13. Comparing average amounts for original and retrofitted frames.

8. Conclusions

In the present research, the fragility of a reinforced concrete building is estimated before and after retrofitting with CBF, EBF and BRB. Fragility curves in the PGA system are also developed with the use of nonlinear time history analysis to study the effect of different brace types. Bi-parametric lognormal distribution functions are also employed to elucidate fragility curves. These fragility curves are utilized in correspondence with the damage scales relevant to the reinforced concrete building under study. Moreover, these fragility curves also serve to determine the potential seismic damage and to evaluate the effect of different brace types in the retrofitting process. It can be concluded that:

- Simulated fragility curves exhibit improvement on the PGA scale after being retrofitted with braces.
- As the analysis of the curves elucidates, brace distribution affects the reliability of seismic performance of the retrofitted frames. From among different brace distribution types, the three models of C3, B3 and E3 are more trustworthy in seismic activities than the rest of their circle. The reason is that in these three models, the load is evenly and symmetrically distributed and the braces are placed at maximum space from one another in the mid-rise RC frames.
- Regarding the fragility curves of each model, it is evident that Buckling Restrained Braces (BRB) have a better effect in seismic retrofitting.
- Finally, eccentrically braced frames also show better resistance than concentrically braced frames, for they absorb higher amounts of seismic energy.
- What is more, from among the two damage scales of ‘inter-story drift’ and ‘plastic axial deformation’, the latter is more useful in developing fragility curves for bracing elements. It should be taken into account that, inter-story drift is often regarded as a parameter of the function of the system, while plastic axial deformation is considered the parameter of the function of the element. So it is natural that they do not yield similar seismic fragility amounts.

References

1. Al-Zand, A.W.; Badaruzzaman, W.H.W.; Mutalib, A.A.; and Hilo, S.J. (2017). Modelling the delamination failure along the CFRP-CFST beam interaction surface using different finite element techniques. *Journal of Engineering Science and Technology* (*JESTEC*), 12(1), 214-228.
2. Khelifa, M.; and Celzard, A. (2014). Numerical analysis of flexural strengthening of timber beams reinforced with CFRP strips. *Journal of Composite Structures*, 111, 393-400.
3. Youssef, O.; ElGawady, M.A.; and Mills, J.E. (2016). Static cyclic behaviour of FRP-confined crumb rubber concrete columns. *Engineering Structures*, 113, 371-387.
4. Allahyari, H.; Dehestani, M.; HosseynaliBeygi, M.; NavayiNeya, B.; and Rahmani, E. (2014). Mechanical behavior of steel-concrete composite decks with perfobond shear connectors. *Journal of Steel and Composite Structures*, 17(13), 339-358.
5. Naghipour, M.; Nematzadeh, M.; and Yahyazadeh, Q. (2011). Analytical and experimental study on flexural performance of WPC_FRP beams. *Journal of Construction and Building Materials*, 25(2011), 829-837.
6. Di Sarno, L.; and Elnashai, A.S. (2009). Bracing systems for seismic retrofitting of steel frames. *Journal of Constructional Steel Research*, 65(2), 452-465.
7. Tan. H.; Huang, L.; Yan, L.; Yi, H.; and Tian, X. (2014). Seismic behavior of newly constructed three-bay steel X-braced RC space frame. *Journal of Earthquake and Tsunami*, 8(4), 1-17.
8. Nazri, F.M.; and Yan, P.S. (2014). Seismic performance of moment-resisting concrete Frames subjected to earthquake excitation. *Journal of Engineering Science and Technology*, 9(6), 717-727.
9. GhodratiAmiri, G.; Jamnani, H.H.; and Ahmadi H.R. (2009). The effect of analysis methods on the response of steel dual-system frame buildings for seismic retrofitting. *International Journal of Engineering*, 22(4), 317-331.
10. Parsaeifard, N.; and Nateghi, F.A. (2012). The effect of local damage on energy absorption of steel frame buildings during earthquake. *International Journal of Engineering-Transactions B: Applications*, 26(2), 143-152.
11. Pagni, C.A.; and Lowes, L.N. (2006). Fragility functions for older reinforced concrete beam–column joints. *Journal of Earthquake Spectra*, 22(1), 215-238.
12. Kappos, A.J.; Panagopoulos, G.; Panagiotopoulos, C.; and Penelis, G. (2006). A hybrid method for the vulnerability assessment of RC and URM buildings. *Journal of Bulletin of Earthquake Engineering*, 4(4), 391-413.
13. Jeong, S.-H.; and Elnashai, A.S. (2007). Probabilistic fragility analysis parameterized by fundamental response quantities. *Journal of Engineering Structures*, 29(6), 1238-1251.
14. Lagaros, N.D. (2008). Probabilistic fragility analysis of RC buildings designed with different rules. *Journal of Earthquake Engineering and Engineering Vibrations*, 7(1), 45-56.

15. Kircil, M.S.; and Polat, Z. (2006). Fragility analysis of mid-rise RC frame buildings. *Journal of Engineering Structures*, 28(9), 1335-1345.
16. Miranda, E.; and Akkar, S.D. (2006). Generalized inter story drift spectrum. *Journal of Structural Engineering*, 132(6), 840-852.
17. Thomsen, J.H.; and Wallace, J.W. (1995). Displacement-based design of RC structural wall: an experimental investigation of walls with rectangular and T-shaped cross-sections. *Report No. Cu/Cee-95-06*, Department of Civil and Environmental Engineering at Clark University, USA.
18. Estekanchi, H.; and Arjomandi, K. (2007). Comparison of damage indexes in nonlinear time history analysis of steel moment frames. *Asian Journal of Civil Engineering (building and housing)*, 8(6), 629-646.
19. FEMA 306. (1998). Evaluation of earthquake damaged concrete and masonry wall buildings. *Federal Emergency Management Agency*, Washington, D.C.
20. Standard No. 2800. (1990). Building and housing research center. *Iranian code of practice for seismic resistant design of buildings*, 1st revision, Tehran, Iran.
21. Abdollahzadeh, G.R.; Faghihmaleki, H. (2017). A method to evaluate the risk-based robustness index in blast-influenced structures. *Earthquakes and Structures*, 12(1), 47- 54.
22. Standard No. 2800. (2013). Building and housing research center. *Iranian code of practice for seismic resistant design of buildings*, 4th revision, Tehran, Iran.
23. Iranian National Building Code. (2009). Design and implementation of concrete buildings. *Office of National Building Regulations*, Tehran, Iran.
24. FEMA 356. (2006). Prestandard and commentary for the seismic rehabilitation of buildings. *FEMA-356*, Federal Emergency Management Agency, Washington, D.C.
25. Faghihmaleki, H.; Nejati, F.; Mirzagoltabar-Roshan, A.; and Y. Batebi-Motlagh. (2017). An evaluation of multi-hazard risk subjected to blast and earthquake loads in RC moment frame with shear wall. *Journal of Engineering Science and Technology* (*JESTEC*), 12(3), 636-647.
26. Adiyanto, M.I.; and Majid, T.A. (2014). Seismic design of two storey reinforced concrete building in Malaysia with low class ductility. *Journal of Engineering Science and Technology* (*JESTEC*), 9(1), 27-46.
27. Abdollahzadeh, G.R.; and Faghihmaleki, H. (2014). Response modification factor of SMRF improved with EBF and BRBs. *Journal of Advanced Research in Dynamical and Control Systems*, 6(4), 42-55.
28. Sabeli, R.; Mahin, S.; and Chang, C. (2003). Seismic demand on steel braces frame building with buckling restrained braces. *Journal of Engineering Structures*, 25(5), 655-666.
29. Abdollahzadeh, G.R.; and Banihashemi, M.R. (2013). Response modification factor of dual moment resistant frame with buckling restrained brace (BRB). *Journal of Steel and Composite Structures*, 14(6), 621-636.
30. Mazzolani, F.M. (2008). Innovative metal systems for seismic upgrading of RC structures. *Journal of Constructional Steel Research*, 64(8), 82-95.

31. D'Aniello, M.; Della Corte, G.; and Mazzolani, F.M. (2006). Seismic upgrading of RC buildings by steel eccentric braces. Experimental results vs. numerical modeling. *Proceedings of the 5th International Conference on Behavior of Steel Structures in Seismic Areas*.
32. Next Generation Attenuation, N.G.A. (2005). *Project strong motion* database. Retrieved November 5, 2015, from http://peer.berkeley.edu/nga/.
33. SeismoSoft. (2012). *Seismosignal*. Earthquake engineering software solutions. Version 5.1.0. Retrieved October 5, 2015, from http://www.seismosoft.com/.
34. Symth, A.W.; Altay, G.; Deodatis, G.; Erdik, M.; Franco, G.; and Gülkan, P. (2004). Probabilistic benefit-cost analysis for earthquake damage mitigation: Evaluating measures for apartment houses in Turkey. *Journal of Earthquake Spectra*, 20(1), 171-203.
35. Jamnai, H.H.; Faghihmaleki, H.; and Gholampour, S. (2014). Seismic improvement of reinforced concrete buildings with X-brace by fragility curve. *8th National Congress on Civil Engineering*, Babol Noshirvani University of Technology, Babol, Iran.
36. Abdollahzadeh, G.R.; and Faghihmaleki, H. (2013). Seismic improvement of concrete bending frames with shear-wall and BRB brace. *4th International Conference on Concrete & Development*, Tehran, Iran.
37. Faghihmaleki, H.; Abdollahzadeh, G.; and Jamnani, H.H. (2014). Effect of structure height in seismic fragility curve. *Journal of Applied Mathematics in Engineering, Management and Technology*, 2(6), 498-503.